

Biological characterization of *Euscelidius variegatus* iflavirus 1

Sara Ottati^{a,b,1}, Alberto Persico^{a,b,1}, Marika Rossi^a, Domenico Bosco^b, Marta Vallino^a, Simona Abbà^a, Giulia Molinatto^{a,b}, Sabrina Palmano^a, Raffaella Balestrini^a, Luciana Galetto^{a,*}, Cristina Marzachi^a

^aIstituto per la Protezione Sostenibile delle Piante, Consiglio Nazionale delle Ricerche, IPSP-CNR, Strada delle Cacce 73 10135, Torino, Italy

^bDipartimento di Scienze Agrarie, Forestali ed Alimentari DISAFA, Università degli Studi di Torino, Largo Paolo Braccini 2, 10095, Grugliasco (TO), Italy

sara.ottati@ipsp.cnr.it

albertopersico@hotmail.it

marika.rossi@ipsp.cnr.it

domenico.bosco@unito.it

marta.vallino@ipsp.cnr.it

simona.abba@ipsp.cnr.it

giulia.molinatto@ipsp.cnr.it

sabrina.palmano@ipsp.cnr.it

raffaella.balestrini@ipsp.cnr.it

crisrina.marzachi@ipsp.cnr.it

* Corresponding author

E-mail address: luciana.galetto@ipsp.cnr.it

¹ Equal first author

28

Abstract

29 Virus-based biocontrol technologies are gaining attention as sustainable alternatives to
30 pesticides and insecticides. Phytoplasmas are prokaryotic plant pathogens causing severe
31 losses to crops worldwide. Novel approaches are needed since insecticide treatments against
32 their insect vectors and rogueing of infected plants are the only available strategies to
33 counteract phytoplasma diseases. A new iflavirus, named EVV-1, has been described in the
34 leafhopper phytoplasma vector *Euscelidius variegatus*, rising the hypothesis of virus-based
35 application against phytoplasma disease. Here EVV-1 is characterized in its transmission
36 routes and localization within the host to unfold the mechanism of insect tolerance to virus
37 infection. Both vertical and horizontal transmissions occur, and the former resulted more
38 efficient. The virus is ubiquitously distributed in different organs and life-stages, with the
39 highest loads measured in ovaries and first to third instar nymphs. The basic knowledge
40 gained here on biological viral properties is crucial for future application of iflaviruses as
41 biocontrol agents.

42

43 *Keywords*

44 Leafhopper, phytoplasma vector, insect virus, vertical transmission, horizontal transmission

45

46 1. Introduction

47 The onset of next generation sequencing gave a strong impulse in the last few years to
48 the discovery of many novel viruses in arthropods (Dong et al., 2018; dos Santos et al., 2019;
49 O'Brien et al., 2018; Yang et al., 2019). In particular, this technology resulted crucial for the
50 identification of covert viruses, which display no overtly pathological effects on their hosts
51 (Nouri et al., 2018). Within the newly discovered viral entities, positive-sense RNA viruses are
52 preponderant (Bonning, 2020). Among them, iflaviruses form a distinct group in the order
53 *Picornavirales*, justifying their classification in the virus family *Iflaviridae* (Van Oers, 2010).
54 Interestingly, some of these viruses may cause developmental anomalies (Li et al., 2019)
55 behavioural alterations (Wells et al., 2016), histopathological effects (Brettell et al., 2017), and
56 premature death (Geng et al., 2017) of the insect host, while others do not cause any evident
57 symptoms (dos Santos et al., 2019; Murakami et al., 2013; Yang et al., 2019). Transmission
58 modalities of these viruses have been explored, leading however to a multifaceted, not
59 univocal infection model. In some cases, horizontal transmission (oral route) is the most
60 efficient spreading way, such as for *Nilaparvata lugens* honeydew virus-1 of the brown
61 leafhopper (Murakami et al., 2013) and for *Helicoverpa armigera* iflavirus (Yuan et al., 2017)
62 and Nora Virus (Yang et al., 2019) of the cotton bollworm. Similarly, the horizontal route is
63 the main transmission modality for *Pyrrhocoris apterus* virus 1 in red firebugs (Vinokurov
64 and Koloniuk, 2019). On the contrary, vertical transmission (from infected parental
65 specimens to progeny) better explains viral spreading in the cases of the causal agent of
66 *Antheraea pernyi* Vomit Disease of Chinese oak silkworm (Geng et al., 2017) and for the
67 *Spodoptera exigua* iflaviruses-1 and 2 of the beet armyworm (Virto et al., 2014). In the case of
68 Deformed Wing Virus (DWV) of the honeybee both the horizontal route, through *Varroa*
69 *destructor* mite as vector, and the vertical viral transmission occur (Chen et al., 2006; Martin
70 and Brettell, 2019; Yue, 2005).

71 The genomic features, phylogenetic analysis, and prevalence of a new member of the
72 family *Iflaviridae*, named *Euscelidius variegatus* virus 1 (EVV-1), have been reported (Abbà et
73 al., 2017) as additional result obtained during the *de novo* assembly of transcriptome from the
74 hemipteran leafhopper *Euscelidius variegatus* Kirschbaum (Galletto et al., 2018). EVV-1 does
75 not induce any evident symptom in the *E. variegatus* surveyed population, which is laboratory
76 reared, and shows a viral endemic infection (100% prevalence) (Abbà et al., 2017). EVV-1
77 forms non-enveloped, icosahedral particles, and the ssRNA(+) genome encodes a single
78 polyprotein of 3132 amino acids, which is post-translationally processed. *Euscelidius*
79 *variegatus* (Cicadellidae: Deltocephalinae) is a palearctic, multivoltine and polyphagous
80 species, widespread in Europe and North America. High relevance is given to this species
81 since it is a natural vector of the 'Candidatus *Phytoplasma asteris*' (chrysanthemum yellows
82 strain) and a laboratory vector of the Flavescence dorée phytoplasma (Caudwell et al., 1972;
83 Rashidi et al., 2014). Phytoplasmas are plant-pathogenic bacteria that cause severe symptoms
84 to affected plants, leading to heavy economic losses to many crops worldwide (Tomkins et al.,
85 2018). In particular, Flavescence dorée phytoplasma of grapevine is a quarantine pest, which
86 strongly limits European viticulture (EFSA Panel on Plant Health (PLH), 2014; EFSA Panel on
87 Plant Health (PLH) et al., 2016). Phytoplasmas are obligate parasites and display a dual life
88 cycle, infecting phloem of host plant as well as insect vector body. Several lines of evidence
89 indicate that interactions between phytoplasmas and vector host cells are very strict and may
90 regulate transmission ability (Arricau-Bouvery et al., 2018; Galletto et al., 2011; Rashidi et al.,
91 2015; Suzuki et al., 2006; Trivellone et al., 2019). Indeed, molecular relationships between
92 pathogens and insect hosts contribute to determining phytoplasma transmission specificity,
93 together with plant susceptibility, as well as feeding behaviour, ecological dispersal and plant
94 host range preference of vectors (Bosco and D'Amelio, 2010; Sugio et al., 2011). Insects play a

95 key role in phytoplasma epidemiology and therefore the main control strategies to limit these
96 pathogens are the insecticide treatments against vector species (Marcone, 2014).

97 The urgent need for more targeted and sustainable pest management approaches in
98 fighting against phytoplasma diseases encourages the exploration of new research frontiers to
99 envisage potential innovative use of biocontrol agents, such as insect viruses. Nevertheless,
100 many fundamental biological features of EVV-1 were unknown, impairing any potential
101 applications of this agent in biocontrol strategy or as VIGS vector. To fill the gap of knowledge
102 of EVV-1 biology, we investigated here the presence of EVV-1 virus in different developmental
103 stages and organs of *E. variegatus*, as well as both horizontal and vertical transmission of this
104 iflavivirus among insect populations.

105

106 2. Materials and methods

107 2.1 Insects

108 *Euscelidius variegatus* of the Turin laboratory colonies were originally collected in
109 Piedmont (Italy) and reared on oat, *Avena sativa* (L.), inside plastic and nylon cages in growth
110 chambers at 20–25 °C with a L16:D8 photoperiod. A French population of *E. variegatus* was
111 kindly provided by Dr. Xavier Foissac (INRA, UMR1332 Biologie du Fruit et Pathologie,
112 Bordeaux, France) and reared in Turin laboratory under the above described conditions. The
113 former population, hereinafter referred as EvaTo, was naturally infected with EVV-1 virus
114 with a 100% prevalence, whereas the latter, hereinafter EvaBx, resulted EVV-1 free, according
115 to molecular detection and electron microscopy observation (Abbà et al., 2017). The two
116 colonies were routinely confirmed to be EVV-1 infected (EvaTo) and free (EvaBx) by RT-qPCR,
117 as described below.

118 2.2 Collection of different insect life stages and organ dissection

119 To determine the viral abundance in different insect life stages, total RNAs were
120 extracted from laid eggs, I-V instar nymphs and adults of virus infected EvaTo population.
121 Preliminary experiments showed that egg collection was easier when eggs were laid on
122 *Arabidopsis thaliana* plants than on *A. sativa* or *Vicia faba* plants. Therefore, about 100 EvaTo
123 female adults were caged on 15 *A. thaliana* plants for four days and then eggs were collected
124 with sterile forceps under a stereomicroscope. Seven pooled samples, each made of about 30
125 laid eggs, were obtained. To exclude surface viral contamination, egg samples were sterilized
126 according to Prado et al. (2006) and then stored at -80°C prior to RNA extraction. For every
127 nymphal stage, 10 pooled samples (each with three EvaTo specimens) were collected and
128 stored at -80°C until RNA extraction. Newly emerged EvaTo adults (five males and five
129 females) were also collected and stored.

130 To estimate the viral presence in different insect organs, total RNAs were extracted
131 from Malpighian tubules, salivary glands, guts, ovaries, testes and hemolymph of newly
132 emerged EvaTo adults. Three hemolymph samples (each with hemolymph collected from 10
133 specimens) were obtained by removing the head of a CO₂-anaesthetized adult and sucking 0.5
134 µL from the inner thorax cavity with a Cell Tram Oil microinjector (Eppendorf), under a
135 stereomicroscope. For the remaining organs, three pooled samples (each made of five
136 dissected organs) were obtained. Organs were carefully separated with forceps and needles
137 under a stereomicroscope, rinsed with phosphate-buffered saline (PBS) solution and stored at
138 -80°C until RNA extraction.

139

140 *2.3 Virus vertical transmission route test*

141 To determine whether EVV-1 is vertically transmitted, virus free EvaBx adults were
142 injected with a fresh extract of EvaTo individuals. Microinjection was chosen as infection
143 modality to maximize the probability to obtain a high number of infected EvaBx adults. These
144 were then used as F0 parents to test vertical transmission to the offspring (F1 generation).
145 The fresh extract containing virus particles was prepared by crushing 30 EvaTo adults in 900
146 μL of cold filter-sterilized injection buffer (300 mM glycine, 30 mM MgCl_2 , pH 8.0) as detailed
147 by Bressan et al. (2006). The extract was clarified by slow centrifugation (10 min, 800 g), and
148 passed through a 0.22 μm pore-size filter. All extraction steps were done at 4°C. Newly
149 emerged EVV-1 free EvaBx adults were CO_2 anaesthetized and injected with 0.5 μL of virus
150 containing solution between two abdominal segments under a stereomicroscope with a Cell
151 Tram Oil microinjector (Eppendorf). As negative control, a group of EvaBx insects was
152 injected with injection buffer only. Injected insects were isolated on fresh oat plants and
153 sampled at 4 and 10 days post injection (dpi). The F1 adults were collected, at 60 dpi. All
154 collected insects (F0 and F1) were stored at -80°C until RNA extraction to check the presence
155 of EVV-1. The experiment was repeated twice.

156 *2.4 Virus horizontal transmission route test*

157 Initially, to determine whether EVV-1 is horizontally transmitted, EVV-1 free EvaBx
158 adults were caged together with infected EvaTo. In order to distinguish individuals belonging
159 to the two original populations, three strategies were carried out: EvaBx third instar nymphs
160 were caged together with EvaTo adults (Experiment 1); EvaBx female adults were caged with
161 EvaTo male adults (Experiment 2); and EvaBx male adults were caged with EvaTo female
162 adults (Experiment 3). For each experiment, 50 EvaBx insects were co-fed on the same oat
163 plant together with 50 EvaTo individuals for two weeks, then transferred to a new plant in a
164 new clean cage (rinsed with commercial bleach and water) and sampled three weeks later for
165 RNA extraction and virus detection. Each experiment was repeated twice.

166 After the positive results of co-feeding, three possible horizontal transmission
167 modalities were specifically tested i) fecal-oral route, ii) virus infection via plant, and iii)
168 cuticle penetration. Fecal-oral transmission modality was assessed according to Murakami et
169 al. (2013). About 60 EvaTo adults were confined within a 50-mL conical tube for 1 h. The
170 insects were then removed from the tube, and the excreted honeydews were collected by
171 rinsing the wall of the plastic tube with 4 mL of artificial feeding medium (5% sucrose, 10 mM
172 Tris/Cl, 1 mM EDTA, pH 8.0 (Rashidi et al., 2015)). An aliquot (400 μL) of this solution was
173 stored at -80°C for RNA extraction to confirm the presence of the virus, while the remaining
174 solution was used to artificially feed EvaBx adults. To this purpose, non-viruliferous insects
175 were confined within small chambers according to Rashidi et al. (2015). Six small cages were
176 set up, each with five EvaBx insects allowed to feed for 48h on 600 μL of honeydew solution
177 laid between two layers of stretched Parafilm. As negative controls, three small cages were set
178 up with artificial medium only, devoid of honeydew. Following artificial feeding, alive insects
179 were caged on oat plants for ten days (Murakami et al., 2013), then collected and stored at -
180 80°C, until RNA extraction for virus detection. To assess the plant-mediated horizontal
181 transmission of EVV-1, virus presence was initially tested in *A. sativa* plants exposed to either
182 EvaTo or EvaBx insects. To determine whether EVV-1 virus is able to invade the plant tissue
183 or only remains on the plant surface, samples from plants exposed to EvaTo insects were
184 surface sterilized (Prado et al., 2006) before RNA extraction and EVV-1 diagnosis. Later on,
185 virus transmission through the host plant was tested by isolating about 50 EvaTo adults for

186 one week on an oat plant. The virus-positive insects were then removed, while the oat plant
187 was used to feed about 50 EvaBx adults for the following week. EvaBx adults were then
188 transferred onto a fresh oat plant and five of them were tested for the presence of EVV-1
189 every seven days for one month. To assess EVV-1 ability to penetrate through the insect
190 cuticle, EvaBx nymphs were submerged into fresh virus extract. For this experiment, second
191 instar nymphs were used, as the highest virus level was detected at this life stage in EvaTo
192 and the insect dimensions allowed an easier manipulation compared to the smaller and more
193 delicate first instar nymphs. Briefly, EvaBx nymphs were CO₂ anaesthetized and submerged
194 for five minutes in 300 µL of fresh virus solution prepared by crushing ten EvaTo adults in
195 400 µL of PBS added with a cocktail of protease inhibitors (Pierce Protease Inhibitor Mini
196 Tablets, EDTA-Free, Thermo Scientific). The extract was clarified by slow centrifugation (5
197 min, 4500 g). Submerged nymphs were then maintained on an oat plant and collected as
198 adults for RNA extraction and virus detection.

199 *2.5 RNA extraction and cDNA synthesis*

200 Total RNAs were extracted from samples of single *E. variegatus* adults, and pooled
201 samples of i) 30 laid eggs, ii) three nymphs, iii) three dissected organs, iv) hemolymph
202 collected from 10 insects, v) honeydew collected from 60 insects and vi) 500 mg of oat leaves.
203 The samples were frozen with liquid nitrogen, crushed with a micropestle in sterile
204 Eppendorf tubes, and homogenized in Tri-Reagent (1 mL for plant samples and 0.5 mL for all
205 other samples). Samples were centrifuged 1 min at 12.000 g at 4°C and RNAs were extracted
206 from supernatants with Direct-zol RNA Mini Prep kit (Zymo Research), following
207 manufacturer's protocol and including the optional DNase treatment step. Concentration,
208 purity, and quality of extracted RNA samples were analysed through a Nanodrop
209 spectrophotometer (Thermo Scientific). For each sample, cDNA was synthesized from total
210 RNA (1 µg) with random hexamers using a High Capacity cDNA reverse transcription kit
211 (Applied Biosystems). Yields of reverse transcription reactions were estimated by reading a
212 1:10 cDNA dilution in a Nanodrop spectrophotometer (Thermo Scientific).

213 *2.6 EVV-1 qPCR assays and statistical analyses*

214 A multiplex qPCR assay was developed to detect and quantify virus presence in *E.*
215 *variegatus* adults. To detect EVV-1, primers and FAM-labelled TaqMan probe were designed
216 on the virus capsid 1 coding sequence (Evv1Cap1Fw 5'-GACCATTATCGCGCTAATG-3',
217 Evv1Cap1Rv 5'-AGTGCTCATCATAGGACA-3', Evv1Cap1Probe 5'-FAM-
218 ATTCTCGTAGCCAACACTGCCAAAC-3'). To check that all the cDNA samples were properly
219 amplifiable, the *E. variegatus* glyceraldehyde-3-phosphate dehydrogenase (GAPDH) transcript,
220 was chosen as endogenous control. To amplify the insect GAPDH, the primer GapFw632 (5'-
221 ATCCGTCGTCGACCTTACTG-3' (Galletto et al., 2013)), was used with the newly designed
222 primer GapRv819 (5'-GTAGCCCAGGATGCCCTTC-3') and the internal HEX-labelled TaqMan
223 probe GapEvProbe (5'-HEX-ATATCAAGGCCAAGGTCAAGGAGGC-3'). One µL of cDNA was used
224 as template in a reaction mix of 10 µL total volume, containing 1X iTaq Universal Probes
225 Supermix (Bio-Rad), 200 nM of each of the four primers and 300 nM of each of the two
226 TaqMan probes. Each sample was run in triplicate in a CFX Connect Real-Time PCR Detection
227 System (Bio-Rad). Cycling conditions were 95°C for 3 min and 40 consecutive cycles at 95°C
228 for 10 s as denaturing step followed by 30 s at 60°C as annealing/extension step. In each qPCR
229 plate, four serial 100-fold dilutions of pGem-T Easy (Promega) plasmids, harbouring the
230 target virus and insect genes, were included to calculate the viral load. For both plasmid
231 standard curves, dilutions included in plates ranged from 10⁸ to 10² target copy numbers per
232 µL and were prepared taking into account that 1 fg of plasmids harbouring EVV-1 and GAPDH

233 gene portions contains 138 and 244 number of molecules, respectively. Dilution series of both
234 plasmids were used to calculate qPCR parameters (reaction efficiency and R^2). Mean virus
235 copy numbers in amplified samples were automatically calculated by CFX Maestro™
236 Software (Bio-Rad) and used to express virus amount as EVV-1 copy numbers/insect GAPDH
237 transcript.

238 For comparison of viral abundance within different insect life stages and organs, virus
239 load was expressed as EVV-1 copy numbers/ng of cDNA, as GAPDH transcript levels varied
240 among the different organs and life stages (Supplementary Tables S1 and S2).

241 SigmaPlot version 13 (Systat Software, Inc., www.systatsoftware.com.) was used for
242 statistical analyses. To compare viral load among different categories (life stages, organs and
243 vertical transmission experiments) ANOVA, followed by the proper post hoc test, or Kruskal
244 Wallis test, when the parametric analysis assumptions were not met, were used. To compare
245 viral load between two groups of samples (male vs. female EvaTo adults, virus exposed EvaBx
246 vs. EvaTo samples in horizontal transmission experiments) t-test was used.

247

248 3. Results

249 3.1 EVV-1 qPCR diagnostic and quantitative assay

250 A multiplex qPCR assay was optimized to detect and quantify the EVV-1 virus in *E.*
251 *variegatus* adults, using primers and TaqMan probes targeting viral EVV-1 capsid 1 and insect
252 GAPDH coding sequences. The viral genomic portion coding the virus capsid 1 protein was
253 selected to maximize the specificity of EVV-1 detection, as this genomic portion was poorly
254 conserved among other iflaviruses according to BLAST analysis (not shown). Standard curves
255 of plasmids harbouring viral and insect target amplicons showed 96.5 and 103.1% qPCR
256 efficiencies, respectively, with a 0.998 R^2 for both curves. The most diluted standard point
257 (10^2 copy numbers/ μ L) was detected before the 35th amplification cycle by both viral and
258 insect primer sets. The test successfully detected EVV-1 in single EvaTo individuals (n=10),
259 whereas no amplification was obtained from any of the 10 tested EvaBx. Quantification of
260 EVV-1 in the EvaTo adults ranged from 0.21 to 0.84 EVV-1 copy numbers/insect GAPDH
261 transcript.

262 3.2. EVV-1 distribution in different insect life stages and organs

263 EVV-1 was detected in the eggs and all the insect developmental stages (I-V instar
264 nymphs and adults) of EvaTo population. Male and female EvaTo individuals were considered
265 together for the analyses, as no significant differences were found between their viral loads (t-
266 test $t=1.448$, $P=0.186$) (Supplementary Table S1). Significant differences were found among
267 developmental stages (ANOVA $F=10.367$, $P<0.001$) and I, II, III instar nymphs showed the
268 highest viral loads, as indicated by pairwise multiple comparison according to Duncan's
269 multiple range test (Fig. 1 and Supplementary Table S1).

270 EVV-1 was detected in all the collected insect organs (Malpighian tubules, salivary
271 glands, guts, ovaries, testes, and hemolymph) of EvaTo population. Viral loads ranged from
272 8606 in the ovaries to 1 EVV-1 copy numbers/ng of cDNA in the testes. The high viral load
273 found in ovaries significantly differed from that found in the testes (ANOVA on Ranks,
274 Kruskal-Wallis test $H=15.415$, $P=0.009$), (Fig. 2 and Supplementary Table S2).

275 3.3 Vertical transmission

276 Virus injection was selected as the most effective infection modality to obtain a high
277 number of newly infected EvaBx individuals (F0) and test their ability to transmit the virus to
278 progeny (F1). Virus presence was detected in 95 and 100 % injected insects sampled at 4 and
279 10 dpi, respectively, as well as in all the F1 tested insects (Supplementary Table S3),
280 demonstrating that vertical viral transmission occurs with very high frequency. Interestingly,
281 mean EVV-1 loads measured in F1 samples were significantly higher than those detected in
282 injected F0 insects sampled at 4 dpi and in EvaTo adults (ANOVA on Ranks, Kruskal-Wallis
283 test $H=15.999$, $P=0.001$) (Fig. 3). The virus was detected in EvaTo fresh extract injected in
284 EvaBx specimens, while no amplification was obtained from EvaBx adults injected with buffer
285 only (negative control).

286 *3.4 Horizontal transmission*

287 The co-feeding experiment, in which EvaTo insects were isolated together with EvaBx
288 specimens on the same plant, indicated that horizontal viral transmission may occur. The
289 overall mean rate of virus transmission was 8.0% (6/75), comprehensively considering the
290 three different co-feeding experimental approaches (indicated in Table 1). The mean viral
291 load, measured in the infected EvaBx insects three weeks after co-feeding with EvaTo, was
292 0.23 EVV-1 copy numbers/insect GAPDH transcript ± 0.10 (SEM, $N=6$), with values ranging
293 from $6.27E-04$ to $5.94E-01$. The mean viral load measured in these virus-exposed EvaBx
294 samples did not significantly differ from that measured in EvaTo adults, which was 0.44 EVV-
295 1 copy numbers/insect GAPDH transcript ± 0.14 (SEM, $N=10$) (t-test $t=1.815$, $P=0.091$).

296 When exploring the possible routes of EVV-1 horizontal transmission, none of the
297 EvaBx insects artificially fed on virus-infected honeydew solution resulted positive for EVV-1
298 presence (Table 1). Therefore, despite the presence of EVV-1 in EvaTo honeydew was
299 confirmed by qPCR, the possibility of virus transmission via fecal-oral route could not be
300 confirmed under our experimental conditions.

301 None of the 20 analysed EvaBx adults tested positive for EVV-1 presence (Table 1),
302 following isolation on *A. sativa* plants that were exposed to EvaTo insects, thus excluding the
303 plant as efficient transmission route. Indeed, while EVV-1 was detected only in one out of six
304 samples of *A. sativa* exposed to EvaTo insects, the virus was absent from all the six analysed
305 plants following surface sterilization of the leaf before RNA extraction, indicating that viral
306 contamination of the leaves may occur. The absence of EVV-1 in plants exposed to EvaBx
307 insects was also confirmed, as expected (0 positive samples out of six total analysed samples).

308 Viral transmission through insect cuticle of second instar EvaBx nymphs occurred in
309 9.5% of the treated insects (Table 1). The viral loads measured in these infected EvaBx insects
310 ranged from 0.09 to 1.79 EVV-1 copy numbers/insect GAPDH transcript. No significant
311 differences were found between the mean viral loads measured in these virus-exposed EvaBx
312 samples and those measured in EvaTo adults (t-test $t=-1.414$, $P=0.174$).

313

314 **4. Discussion**

315 In this work, distribution and transmission routes of the *Euscelidius variegatus*
316 iflavirus 1 were explored to show that the virus is ubiquitous in the insect body and life stages,
317 and it is vertically transmitted to offspring with high efficiency. Unveiling these biological
318 parameters is a prerequisite to explore the potential application of iflaviruses as biocontrol
319 agents of phytoplasma vectors. This work also paves the road to exploit iflaviruses as

320 molecular tools to study insect genes involved in pathogen transmission through the
321 construction of infectious viral clones.

322 Iflaviruses have different ways of colonizing their arthropod hosts. In some cases,
323 viruses do not show tropism for specific organs or tissues, such as the Deformed Wing Virus
324 (DWV) and *Antheraea pernyi* Iflavirus (ApIV). These can be detected in all parts of the bee
325 body, DWV (Martin and Brettell, 2019), or in the head, epidermis, hemocytes, gut, fat body,
326 ovary and testis of the Chinese oak silkworm, ApIV (Geng et al., 2017). On the contrary, other
327 iflaviruses show some organ tropism, such as the Nora Virus of the cotton bollworm (Yang et
328 al., 2019) or the *Helicoverpa armigera* iflavirus (Yuan et al., 2017), which show higher
329 abundance in midgut tissues or higher prevalence in fat bodies compared to other insect body
330 districts, respectively. Molecular analysis showed that EVV-1 is present in different *E.*
331 *variegatus* tissues and organs as well as in different life stages (from egg to adult). The
332 significantly highest viral load detected in I-III instar nymphs may indicate that these stages
333 are probably supporting the peak of viral replication. Indeed, over-time increase of viral load
334 has been observed in pupae of the Chinese oak silkworm following the injection of ApIV
335 purified particles (Geng et al., 2017). Analogously, the high viral load measured in ovaries
336 suggests a key role of this organ in the viral replication cycle. Indeed, this feature may be
337 common to iflaviruses infecting Hemiptera, as the *Laodelphax striatellus* Iflavirus 1 (LsIV1) is
338 present in eggs and ovaries of the small brown planthopper (Wu et al., 2019). Evidence from
339 different iflaviruses seems therefore to delineate an assorted model of insect body
340 colonization, that requires case-by-case characterization.

341 Under our experimental conditions, EVV-1 was efficiently transmitted to the offspring,
342 and complete colonization of the virus-free population occurred in one generation. Vertical
343 transmission is a second common feature between EVV-1 and LsIV1 (Wu et al., 2019). Indeed,
344 following injection of virus-free parents, the newly infected F1 progeny always showed 100%
345 EVV-1 incidence. The development of an efficient multiplex fluorescent qPCR assay, based on
346 glyceraldehyde-3-phosphate dehydrogenase (GAPDH) as an endogenous gene for
347 normalization of quantitative data and as internal control of cDNA quality, allowed the
348 quantitative detection of EVV-1, a prerequisite to characterize its distribution and
349 transmission modalities. Interestingly, the mean viral load of the F1 individuals was
350 significantly higher than that of naturally infected *EvaTo* adults. This result supports the
351 hypothesis of a higher viral replication rate in the experimentally infected than in the
352 naturally infected insects, in the absence of evident fitness costs. Indeed, in several mosquito
353 species, a state of tolerance response against covert arboviral infections has been described
354 leading to persistent infection in the host with few fitness costs (Goic et al., 2016).

355 Horizontal transmission has also been reported for some iflaviruses (Murakami et al.,
356 2013; Yuan et al., 2017), and indeed, it occasionally occurred for EVV-1 under our
357 experimental conditions, although less efficiently than vertical route. In particular, the
358 *Nilaparvata lugens* iflavirus 1 (NHLV-1) is efficiently transmitted to virus-free brown
359 leafhoppers through feeding on infected honeydews (Murakami et al., 2013). On the other
360 hand, despite consistent EVV-1 presence in *EvaTo* honeydew added to the artificial diet, the
361 virus was not transmitted to *EvaBx* individuals through feeding, suggesting this virus is not
362 able to cross the gut barrier. EVV-1 could be sporadically detected in not-sterilized leaves
363 from plants exposed to virus-infected insects, probably due to honeydew contamination, but it
364 was never detected after sterilization of leaf surface. Consistently, the phloem feeding habit of
365 *E. variegatus* may explain its inability to acquire EVV-1 through the host plant.

366 Silencing of insect genes by RNA interference is a promising approach to control insect
367 pests, and it has been applied to several Hemipteran species, among which aphids (Yu et al.,
368 2016), psyllids (Lu et al., 2019), and whiteflies (Shi et al., 2019). Efficient delivery of RNA
369 interfering molecules is difficult to achieve for phloem feeders, and microinjection (Mutti et al.,
370 2006) or plant-mediated silencing strategies (Jaubert-Possamai et al., 2007; Pitino et al.,
371 2011) have been explored. In particular, soaking of nymphs of the psyllid *Diaphorina citri*,
372 vector of '*Candidatus Liberibacter solanacearum*', in a solution containing dsRNA silencing
373 molecules provides efficient silencing of different target genes (Killiny et al., 2014; Yu et al.,
374 2017). Interestingly, EVV-1 could be transmitted to nymphs following their immersion in a
375 solution containing the virus, suggesting that the viral particles are able to penetrate the
376 nymphal cuticle and then replicate in the insect body. This soaking-based strategy of viral
377 delivery may be further explored as a high-throughput technique to increase the horizontal
378 transmission efficiency of phloem feeder viruses. Also, the ability of EVV-1 to penetrate the
379 nymphal cuticle may also explain the occasional transmission of the virus to some EvaBx
380 individuals, following co-feeding together with virus infected EvaTo individuals. In conclusion,
381 both vertical and cuticle horizontal transmission routes may justify the 100% EVV-1
382 prevalence observed in the mass reared EvaTo lab colony.

383 Although the idea behind the application of entomopathogens as biocontrol agent is
384 more than 60 years old (Steinhaus, 1956), the use of insect-specific viruses in plant protection
385 is lately gaining attention. As an example, nowadays Baculoviruses applications range from
386 fitness decreasing (Gramkow et al., 2010), to synergic approach (Haase et al., 2015) to
387 compete with pathogen acquisition. Iflaviruses may often infect their hosts and transcribe
388 high amounts of their RNAs without inducing visible symptom in the infected population (dos
389 Santos et al., 2019), but in the case of *Spodoptera exigua* larvae, infection with an iflavirus
390 increases the susceptibility of the larvae to a baculovirus occlusion body-based insecticide
391 (Carballo et al., 2017). This intriguing cross-talk among different partners of a complex
392 microbiome has been evoked to justify the lower load of EVV-1 in *E. variegatus* individuals
393 infected with *Flavescence dorée* phytoplasma (Abbà et al., 2017). The urgent need for more
394 precise and sustainable pest management approaches to fight against phytoplasma diseases
395 encourages the exploration of new research frontiers to envisage viruses as biocontrol agents
396 able to compete with phytoplasmas transmission and/or acquisition. This pioneering
397 hypothesis is well supported by the cases of West Nile virus vectored by mosquitoes co-
398 infected with Nhumirim virus (Nouri et al., 2018) or with Wolbachia (Glaser and Meola, 2010),
399 and by the cases of Dengue, Chikungunya, and Plasmodium transmitted by *Aedes* co-infected
400 with Wolbachia (Moreira et al., 2009). Several fundamental biological features of EVV-1 were
401 addressed in this work, in view of an ongoing exploration of this virus to express heterologous
402 genes in *E. variegatus* and regulate the expression of insect genes by virus-induced gene
403 silencing (VIGS). To reach this goal, preliminary results in the synthesis of an EVV-1 infectious
404 clone have been gathered (Marzachi et al., 2019) and RNAi mediated by injection of dsRNA
405 molecules has been proven to work efficiently in *E. variegatus* with a long-lasting effect (Abbà
406 et al., 2019). Elucidating the mechanisms of insect tolerance to iflavirus infection paves the
407 way to conceptualize new anti-vectorial strategies to selectively control plant pathogen-
408 transmitter Hemipteran insects.

409

410 **Author contributions**

411 Concept & financing (LG, SA, CM, DB); Experimental design (LG, MR, CM); Execution
412 (SO, AP, MR, MV, GM); Analysis (SO, MR, LG, CM); Publication (LG, MR, SA, MV, SP, DB, RB, CM).

413 All authors read and approved the final manuscript. The authors declare no competing
414 financial interests.

415

416 Acknowledgments

417 The authors thank Elena Zocca for providing plants for insect rearing, Flavio Veratti for
418 maintenance of insect colonies in Turin and Dr. Xavier Foissac for providing adults of *E.*
419 *variegatus* from his laboratory colony, allowing us to set up a virus-free population.

420 This research was supported by Fondazione Cassa di Risparmio di Torino, Projects
421 Siglofit (RF = 2016-0577) and FOotSTEP (RF = 2018-0678), and by H2020 VIROPLANT
422 Project (Grant Agreement 773567).

423

424 References

425 Abbà, S., Galetto, L., Ripamonti, M., Rossi, M., Marzachì, C., 2019. RNA interference of muscle
426 actin and ATP synthase beta increases mortality of the phytoplasma vector *Euscelidius*
427 *variegatus*. Pest. Manag. Sci. 75, 1425–1434. <https://doi.org/10.1002/ps.5263>

428 Abbà, S., Galetto, L., Vallino, M., Rossi, M., Turina, M., Sicard, A., Marzachì, C., 2017. Genome
429 sequence, prevalence and quantification of the first iflavirus identified in a phytoplasma insect
430 vector. Arch. Virol. 162, 799–809. <https://doi.org/10.1007/s00705-016-3158-3>

431 Arricau-Bouvery, N., Duret, S., Dubrana, M.-P., Batailler, B., Desqué, D., Béven, L., Danet, J.-L.,
432 Monticone, M., Bosco, D., Malembic-Maher, S., Foissac, X., 2018. Variable membrane protein A
433 of flavescence dorée phytoplasma binds the midgut perimicrovillar membrane of *Euscelidius*
434 *variegatus* and promotes adhesion to its epithelial cells. Appl. Environ. Microbiol. 84, 8–17.
435 <https://doi.org/10.1128/AEM.02487-17>

436 Bonning, B.C., 2020. The insect virome: opportunities and challenges. Curr. Issues Molec. Biol.
437 1–12. <https://doi.org/10.21775/cimb.034.001>

438 Bosco, D., D'Amelio, R., 2010. Transmission specificity and competition of multiple
439 phytoplasmas in the insect vector, in: Weintraub, P.G., Jones, P. (Eds.), Phytoplasmas:
440 Genomes, Plant Hosts and Vectors. CABI, Wallingford, UK, pp. 293–308.

441 Bressan, A., Clair, D., Sémétey, O., Boudon-Padieu, E., 2006. Insect injection and artificial
442 feeding bioassays to test the vector specificity of Flavescence dorée phytoplasma. Phytopathol.
443 96, 790–796. <https://doi.org/10.1094/PHYTO-96-0790>

444 Brettell, L., Mordecai, G., Schroeder, D., Jones, I., da Silva, J., Vicente-Rubiano, M., Martin, S.,
445 2017. A comparison of Deformed Wing Virus in deformed and asymptomatic honey bees.
446 Insects 8, 28. <https://doi.org/10.3390/insects8010028>

447 Carballo, A., Murillo, R., Jakubowska, A., Herrero, S., Williams, T., Caballero, P., 2017. Co-
448 infection with iflaviruses influences the insecticidal properties of *Spodoptera exigua* multiple
449 nucleopolyhedrovirus occlusion bodies: implications for the production and biosecurity of
450 baculovirus insecticides. PLoS ONE 12, e0177301.
451 <https://doi.org/10.1371/journal.pone.0177301>

- 452 Caudwell, A., Kuszala, C., Larrue, J., Bachelier, J., 1972. Transmission de la Flavescence dorée
453 de la fève à la fève par des cicadelles des genres *Euscelis* et *Euscelidius*. Ann. Phytopathol. No.
454 hors série, 181–189.
- 455 Chen, Y., Evans, J., Feldlaufer, M., 2006. Horizontal and vertical transmission of viruses in the
456 honey bee, *Apis mellifera*. J. Invertebr. Pathol. 92, 152–159.
457 <https://doi.org/10.1016/j.jip.2006.03.010>
- 458 Dong, Y., Chao, J., Liu, J., Rice, A., Holdbrook, R., Liu, Y., Xu, P., 2018. Characterization of a novel
459 RNA virus from *Nesidiocoris tenuis* related to members of the genus Iflavirus. Arch. Virol. 163,
460 571–574. <https://doi.org/10.1007/s00705-017-3622-8>
- 461 dos Santos, E.R., Trentin, L.B., Ecker, A., Silva, L.A., Borges, M., Mowery, J.D., Ribeiro, B.M.,
462 Harrison, R.L., Ardisson-Araújo, D.M.P., 2019. An iflavirus found in stink bugs (Hemiptera:
463 Pentatomidae) of four different species. Virology 534, 72–79.
464 <https://doi.org/10.1016/j.virol.2019.06.002>
- 465 EFSA Panel on Plant Health (PLH), 2014. Scientific Opinion on pest categorisation of
466 Grapevine Flavescence dorée: Grapevine Flavescence dorée pest categorisation. EFSA Journal
467 12, 3851. <https://doi.org/10.2903/j.efsa.2014.3851>
- 468 EFSA Panel on Plant Health (PLH), Jeger, M., Bragard, C., Caffier, D., Candresse, T.,
469 Chatzivassiliou, E., Dehnen-Schmutz, K., Gilioli, G., Jaques Miret, J.A., MacLeod, A., Navajas
470 Navarro, M., Niere, B., Parnell, S., Potting, R., Rafoss, T., Rossi, V., Urek, G., Van Bruggen, A., Van
471 Der Werf, W., West, J., Winter, S., Bosco, D., Foissac, X., Strauss, G., Hollo, G., Mosbach-Schulz, O.,
472 Grégoire, J., 2016. Risk to plant health of Flavescence dorée for the EU territory. EFSA Journal
473 14, 4603. <https://doi.org/10.2903/j.efsa.2016.4603>
- 474 Galetto, L., Abbà, S., Rossi, M., Vallino, M., Pesando, M., Arricau-Bouvery, N., Dubrana, M.-P.,
475 Chitarra, W., Pegoraro, M., Bosco, D., Marzachi, C., 2018. Two phytoplasmas elicit different
476 responses in the insect vector *Euscelidius variegatus* Kirschbaum. Infect. Immun. 86,
477 IAI.00042-18. <https://doi.org/10.1128/IAI.00042-18>
- 478 Galetto, L., Bosco, D., Balestrini, R., Genre, A., Fletcher, J., Marzachi, C., 2011. The major
479 antigenic membrane protein of “*Candidatus* Phytoplasma asteris” selectively interacts with
480 ATP synthase and actin of leafhopper vectors. PLoS ONE 6, e22571;
481 [10.1371/journal.pone.0022571](https://doi.org/10.1371/journal.pone.0022571). <https://doi.org/10.1371/journal.pone.0022571>
- 482 Galetto, L., Bosco, D., Marzachi, C., 2013. Selection of reference genes from two leafhopper
483 species challenged by phytoplasma infection, for gene expression studies by RT-qPCR. BMC
484 Res. Notes 6, 409. <https://doi.org/10.1186/1756-0500-6-409>
- 485 Geng, P., Li, W., de Miranda, J.R., Qian, Z., An, L., Terenius, O., 2017. Studies on the transmission
486 and tissue distribution of *Antheraea pernyi* iflavirus in the Chinese oak silkmoth *Antheraea*
487 *pernyi*. Virology 502, 171–175. <https://doi.org/10.1016/j.virol.2016.12.014>
- 488 Glaser, R.L., Meola, M.A., 2010. The native Wolbachia endosymbionts of *Drosophila*
489 *melanogaster* and *Culex quinquefasciatus* increase host resistance to West Nile Virus infection.
490 PLoS ONE 5, e11977. <https://doi.org/10.1371/journal.pone.0011977>
- 491 Goic, B., Stapleford, K.A., Frangeul, L., Doucet, A.J., Gausson, V., Blanc, H., Schemmel-Jofre, N.,
492 Cristofari, G., Lambrechts, L., Vignuzzi, M., others, 2016. Virus-derived DNA drives mosquito
493 vector tolerance to arboviral infection. Nat. Commun. 7, 12410.

- 494 Gramkow, A., Perecmanis, S., Sousa, R., Noronha, E., Felix, C., Nagata, T., Ribeiro, B., 2010.
495 Insecticidal activity of two proteases against *Spodoptera frugiperda* larvae infected with
496 recombinant baculoviruses. *Viol. J.* 7, 143. <https://doi.org/10.1186/1743-422X-7-143>
- 497 Haase, S., Sciocco-Cap, A., Romanowski, V., 2015. Baculovirus insecticides in Latin America:
498 historical overview, current status and future perspectives. *Viruses* 7, 2230–2267.
499 <https://doi.org/10.3390/v7052230>
- 500 Jaubert-Possamai, S., Le Trionnaire, G., Bonhomme, J., Christophides, G.K., Rispe, C., Tagu, D.,
501 2007. Gene knockdown by RNAi in the pea aphid *Acyrtosiphon pisum*. *BMC Biotechnol.* 7, 63.
502 <https://doi.org/10.1186/1472-6750-7-63>
- 503 Killiny, N., Hajeri, S., Tiwari, S., Gowda, S., Stelinski, L.L., 2014. Double-stranded RNA uptake
504 through topical application mediates silencing of five CYP4 genes and suppresses insecticide
505 resistance in *Diaphorina citri*. *PLoS ONE* 9, e110536.
506 <https://doi.org/10.1371/journal.pone.0110536>
- 507 Li, Jianghong, Wang, T., Evans, J., Rose, R., Zhao, Y., Li, Z., Li, Jilian, Huang, S., Heerman, M.,
508 Rodríguez-García, C., Banmeke, O., Brister, J., Hatcher, E., Cao, L., Hamilton, M., Chen, Y., 2019.
509 The phylogeny and pathogenesis of Sacbrood Virus (SBV) infection in European honey bees,
510 *Apis mellifera*. *Viruses* 11, 61. <https://doi.org/10.3390/v11010061>
- 511 Lu, Z.-J., Huang, Y.-L., Yu, H.-Z., Li, N.-Y., Xie, Y.-X., Zhang, Q., Zeng, X.-D., Hu, H., Huang, A.-J., Yi,
512 L., Su, H.-N., 2019. Silencing of the chitin synthase gene is lethal to the Asian citrus psyllid,
513 *Diaphorina citri*. *IJMS* 20, 3734. <https://doi.org/10.3390/ijms20153734>
- 514 Marccone, C., 2014. Molecular biology and pathogenicity of phytoplasmas. *Ann. Appl. Biol.* 165,
515 199–221. <https://doi.org/10.1111/aab.12151>
- 516 Martin, S.J., Brettell, L.E., 2019. Deformed Wing Virus in honeybees and other insects. *Annu.*
517 *Rev. Virol.* 6, 092818–015700. <https://doi.org/10.1146/annurev-virology-092818-015700>
- 518 Marzachi, C., Ottati, S., Persico, A., Abbà, S., Rossi, M., Vallino, M., Turina, M., Galetto, L., 2019.
519 Virus biology of *Euscelidius variegatus* iflavivirus 1: towards the production of an infectious
520 viral clone. Presented at the 52nd Annual Meeting of the Society for Invertebrate Pathology,
521 SIP/IOBC, 28 July - 1 August 2019. Valencia, Spain, pp. 76–77.
- 522 Moreira, L.A., Iturbe-Ormaetxe, I., Jeffery, J.A., Lu, G., Pyke, A.T., Hedges, L.M., Rocha, B.C., Hall-
523 Mendelin, S., Day, A., Riegler, M., Hugo, L.E., Johnson, K.N., Kay, B.H., McGraw, E.A., van den
524 Hurk, A.F., Ryan, P.A., O'Neill, S.L., 2009. A *Wolbachia* symbiont in *Aedes aegypti* limits
525 infection with Dengue, Chikungunya, and Plasmodium. *Cell* 139, 1268–1278.
526 <https://doi.org/10.1016/j.cell.2009.11.042>
- 527 Murakami, R., Suetsugu, Y., Kobayashi, T., Nakashima, N., 2013. The genome sequence and
528 transmission of an iflavivirus from the brown planthopper, *Nilaparvata lugens*. *Virus Res.* 176,
529 179–187. <https://doi.org/10.1016/j.virusres.2013.06.005>
- 530 Mutti, N.S., Park, Y., Reese, J.C., Reeck, G.R., 2006. RNAi knockdown of a salivary transcript
531 leading to lethality in the pea aphid, *Acyrtosiphon pisum*. *J. Insect Sci.* 6, 1–7.
532 <https://doi.org/10.1673/031.006.3801>
- 533 Nouri, S., Matsumura, E.E., Kuo, Y.-W., Falk, B.W., 2018. Insect-specific viruses: from discovery
534 to potential translational applications. *Curr. Opin. Virol.* 33, 33–41.
535 <https://doi.org/10.1016/j.coviro.2018.07.006>

- 536 O'Brien, C.A., Hall-Mendelin, S., Hobson-Peters, J., Deliyannis, G., Allen, A., Lew-Tabor, A.,
537 Rodriguez-Valle, M., Barker, D., Barker, S.C., Hall, R.A., 2018. Discovery of a novel iflavirus
538 sequence in the eastern paralysis tick *Ixodes holocyclus*. Arch. Virol. 163, 2451–2457.
539 <https://doi.org/10.1007/s00705-018-3868-9>
- 540 Pitino, M., Coleman, A.D., Maffei, M.E., Ridout, C.J., Hogenhout, S.A., 2011. Silencing of aphid
541 genes by dsRNA feeding from plants. PLoS ONE 6, e25709.
542 <https://doi.org/10.1371/journal.pone.0025709>
- 543 Prado, S.S., Rubinoff, D., Almeida, R.P.P., 2006. Vertical transmission of a pentatomid caeca-
544 associated symbiont. Ann. Entomol. Soc. Am. 99, 577–585. [https://doi.org/10.1603/0013-
545 8746\(2006\)99\[577:VTOAPC\]2.0.CO;2](https://doi.org/10.1603/0013-8746(2006)99[577:VTOAPC]2.0.CO;2)
- 546 Rashidi, M., D'Amelio, R., Galetto, L., Marzachi, C., Bosco, D., 2014. Interactive transmission of
547 two phytoplasmas by the vector insect. Ann. Appl. Biol. 165, 404–413.
548 <https://doi.org/10.1111/aab.12146>
- 549 Rashidi, M., Galetto, L., Bosco, D., Bulgarelli, A., Vallino, M., Veratti, F., Marzachi, C., 2015. Role
550 of the major antigenic membrane protein in phytoplasma transmission by two insect vector
551 species. BMC Microbiol. 15, 193; [10.1186/s12866-015-0522-5](https://doi.org/10.1186/s12866-015-0522-5).
552 <https://doi.org/10.1186/s12866-015-0522-5>
- 553 Shi, X.-B., Wang, X.-Z., Zhang, D.-Y., Zhang, Z.-H., Zhang, Z., Cheng, J., Zheng, L.-M., Zhou, X.-G.,
554 Tan, X.-Q., Liu, Y., 2019. Silencing of odorant-binding protein gene OBP3 using RNA
555 interference reduced virus transmission of Tomato Chlorosis Virus. IJMS 20, 4969.
556 <https://doi.org/10.3390/ijms20204969>
- 557 Steinhaus, E.A., 1956. Microbial control—the emergence of an idea. A brief history of insect
558 pathology through the nineteenth century. Hilg 26, 107–160.
559 <https://doi.org/10.3733/hilg.v26n02p107>
- 560 Sugio, A., MacLean, A.M., Kingdom, H.N., Grieve, V.M., Manimekalai, R., Hogenhout, S.A., 2011.
561 Diverse targets of phytoplasma effectors: from plant development to defense against insects.
562 Ann. Rev. Phytopathol. 49, 175–195. [https://doi.org/10.1146/annurev-phyto-072910-
563 095323](https://doi.org/10.1146/annurev-phyto-072910-095323)
- 564 Suzuki, S., Oshima, K., Kakizawa, S., Arashida, R., Jung, H.-Y., Yamaji, Y., Nishigawa, H., Ugaki, M.,
565 Namba, S., 2006. Interaction between the membrane protein of a pathogen and insect
566 microfilament complex determines insect-vector specificity. PNAS 103, 4252–4257.
567 <https://doi.org/10.1073/pnas.0508668103>
- 568 Tomkins, M., Kliot, A., Marée, A.F., Hogenhout, S.A., 2018. A multi-layered mechanistic
569 modelling approach to understand how effector genes extend beyond phytoplasma to
570 modulate plant hosts, insect vectors and the environment. Curr. Opin. Plant Biol. 44, 39–48.
571 <https://doi.org/10.1016/j.pbi.2018.02.002>
- 572 Trivellone, Ripamonti, M., Angelini, E., Filippin, L., Rossi, M., Marzachi, C., Galetto, L., 2019.
573 Evidence suggesting interactions between immunodominant membrane protein Imp of
574 Flavescence dorée phytoplasma and protein extracts from distantly related insect species. J.
575 Appl. Microbiol. 127, 1801–1813. <https://doi.org/10.1111/jam.14445>
- 576 Van Oers, M., 2010. Genomics and biology of Iflaviruses, in: Johnson, K., Agari, S. (Eds.), Insect
577 Virology. Norfolk, pp. 231–250.

- 578 Vinokurov, K.S., Koloniuk, I., 2019. Discovery and characterization of a novel alphavirus-like
579 RNA virus from the red firebug *Pyrrhocoris apterus* L. (Heteroptera). J. Invertebr. Pathol. 166,
580 107213. <https://doi.org/10.1016/j.jip.2019.107213>
- 581 Virto, C., Navarro, D., Tellez, M.M., Herrero, S., Williams, T., Murillo, R., Caballero, P., 2014.
582 Natural populations of *Spodoptera exigua* are infected by multiple viruses that are
583 transmitted to their offspring. J. Invertebr. Pathol. 122, 22–27.
584 <https://doi.org/10.1016/j.jip.2014.07.007>
- 585 Wells, T., Wolf, S., Nicholls, E., Groll, H., Lim, K.S., Clark, S.J., Swain, J., Osborne, J.L., Haughton,
586 A.J., 2016. Flight performance of actively foraging honey bees is reduced by a common
587 pathogen. Environ. Microbiol. Rep. 8, 728–737. <https://doi.org/10.1111/1758-2229.12434>
- 588 Wu, N., Zhang, P., Liu, W., Cao, M., Massart, S., Wang, X., 2019. Complete genome sequence and
589 characterization of a new iflavirus from the small brown planthopper (*Laodelphax striatellus*).
590 Virus Res. 272, 197651. <https://doi.org/10.1016/j.virusres.2019.197651>
- 591 Yang, X., Xu, P., Yuan, H., Graham, R.I., Wilson, K., Wu, K., 2019. Discovery and characterization
592 of a novel picorna-like RNA virus in the cotton bollworm *Helicoverpa armigera*. J. Invertebr.
593 Pathol. 160, 1–7. <https://doi.org/10.1016/j.jip.2018.11.003>
- 594 Yu, X., Gowda, S., Killiny, N., 2017. Double-stranded RNA delivery through soaking mediates
595 silencing of the muscle protein 20 and increases mortality to the Asian citrus psyllid,
596 *Diaphorina citri*. Pest Manag. Sci. 73, 1846–1853. <https://doi.org/10.1002/ps.4549>
- 597 Yu, X.-D., Liu, Z.-C., Huang, S.-L., Chen, Z.-Q., Sun, Y.-W., Duan, P.-F., Ma, Y.-Z., Xia, L.-Q., 2016.
598 RNAi-mediated plant protection against aphids. Pest Manag. Sci. 72, 1090–1098.
599 <https://doi.org/10.1002/ps.4258>
- 600 Yuan, H., Xu, P., Yang, X., Graham, R.I., Wilson, K., Wu, K., 2017. Characterization of a novel
601 member of genus Iflavirus in *Helicoverpa armigera*. J. Invertebr. Pathol. 144, 65–73.
602 <https://doi.org/10.1016/j.jip.2017.01.011>
- 603 Yue, C., 2005. RT-PCR analysis of Deformed wing virus in honeybees (*Apis mellifera*) and
604 mites (*Varroa destructor*). J. Gen. Virol. 86, 3419–3424. [https://doi.org/10.1099/vir.0.81401-](https://doi.org/10.1099/vir.0.81401-0)
605 0
- 606
- 607
- 608

609

610 **Table**

611 **Table 1.** Detection and quantification results of horizontal transmission of *Euscelidius*
 612 *variegatus* virus 1 (EVV-1) to EVV-1 free EvaBx population. Mean quantification cycles (Cq)
 613 obtained from insect glyceraldehyde-3-phosphate dehydrogenase (GAPDH) qPCR assay
 614 confirmed that all samples were amplifiable.

Virus infection modality	Sample description	N° EVV-1 positive/analysed samples	Mean EVV-1 viral load* ± SEM (N)	Mean Cq ± SEM (N) of GAPDH assay
Co-feeding	EvaBx nymphs + EvaTo adults	3/47	0.27 ± 0.11 (3)	18.93 ± 0.36 (47)
	EvaBx females + EvaTo males	2/17	2.56E-03 ± 1.94E-03 (2)	23.45 ± 0.36 (17)
	EvaBx males + EvaTo females	1/11	0.59 (1)	19.44 ± 0.84 (11)
Fecal-oral route	EvaBx adults fed on EvaTo honeydews	0/12	/	20.30 ± 0.28 (12)
Plant-mediated route	EvaBx adults fed on plant exposed to EvaTo adults	0/20	/	20.79 ± 0.44 (20)
Cuticle penetration	EvaBx nymphs submerged in EvaTo extract	10/105	2639 ± 385 (10)	17.85 ± 0.16 (105)

615 *Viral load expressed as EVV-1 copy numbers/insect GAPDH transcript.

616

617

618 **Figure captions**

619

620 **Figure 1. Distribution of *Euscelidius variegatus* virus 1 (EVV-1) in different insect life stages.**
 621 Different letters indicate significant differences in mean viral loads measured in the sample
 622 groups. First to fifth instar nymphs are indicated by Roman numerals and different life stages
 623 are depicted beneath the graph.

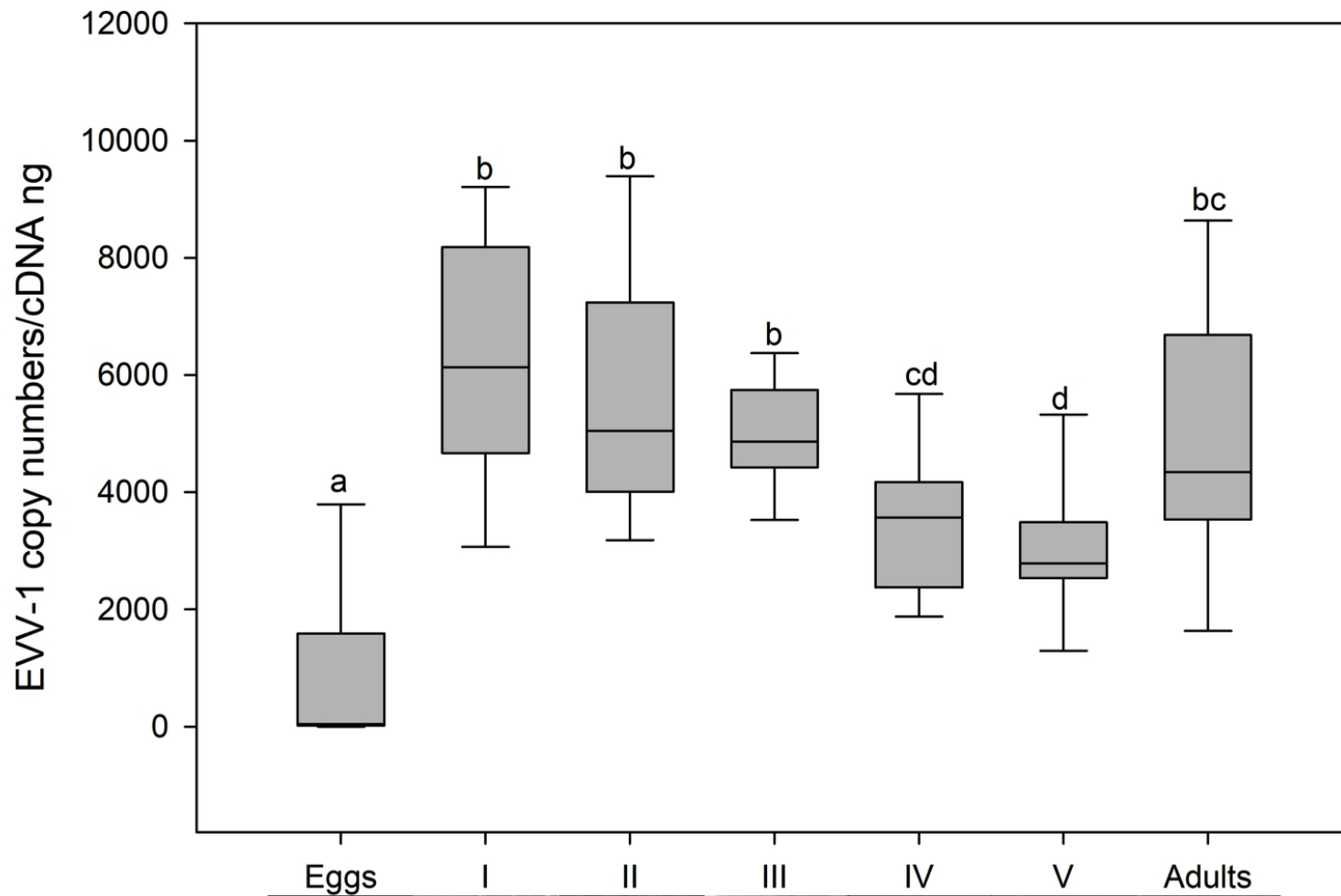
624

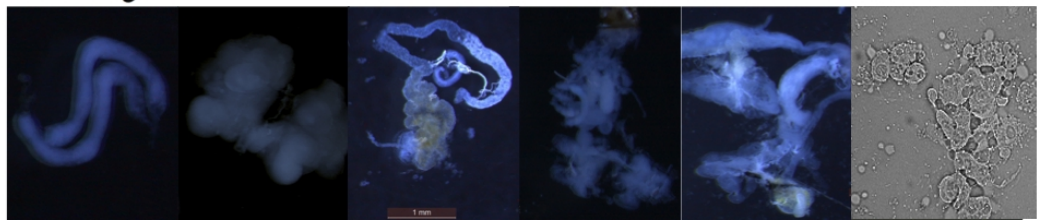
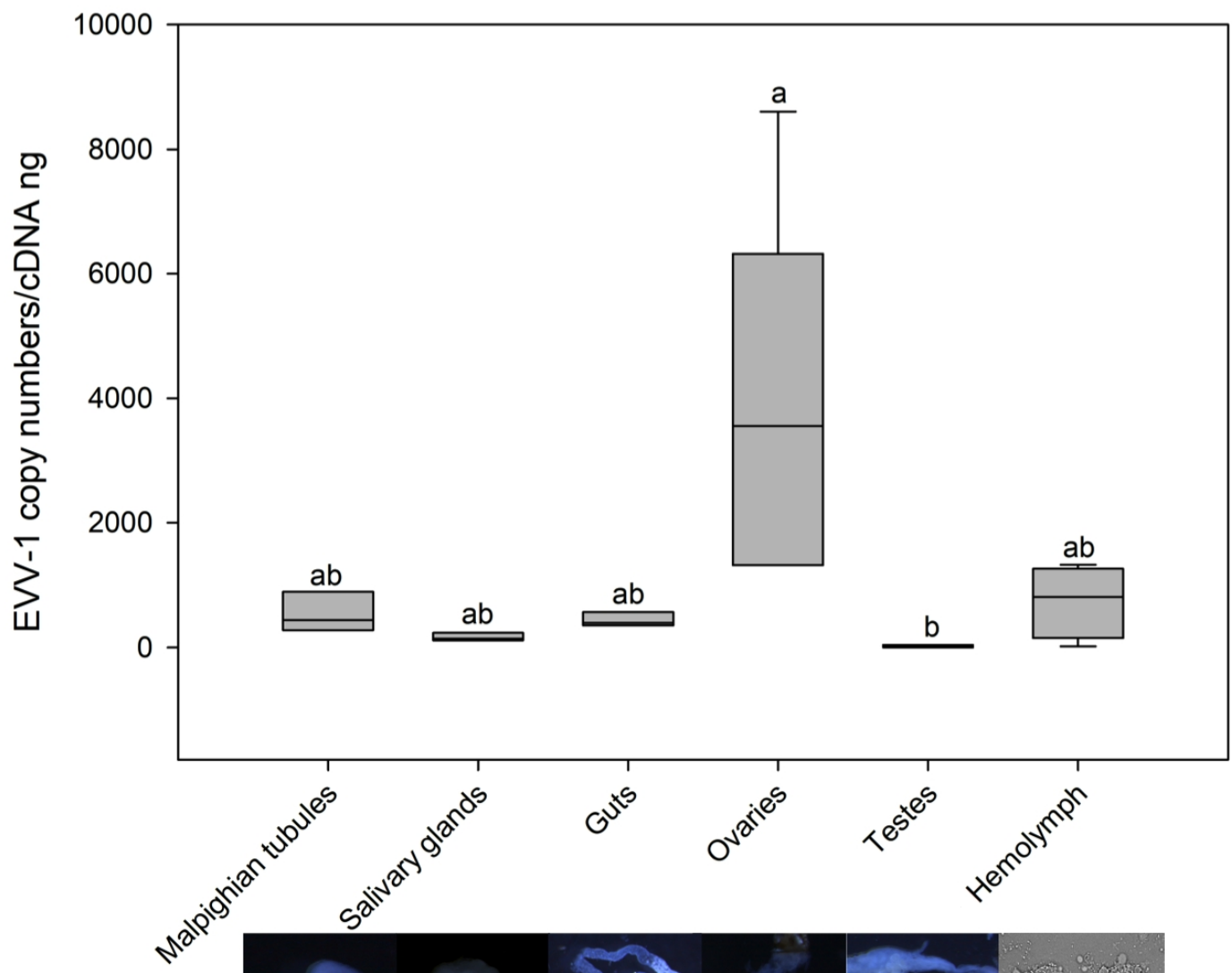
625 **Figure 2. Distribution of *Euscelidius variegatus* virus 1 (EVV-1) in different insect organs.**
 626 Different letters indicate significant differences in mean viral load measured in the sample
 627 groups. The different insect organs are depicted beneath the graph.

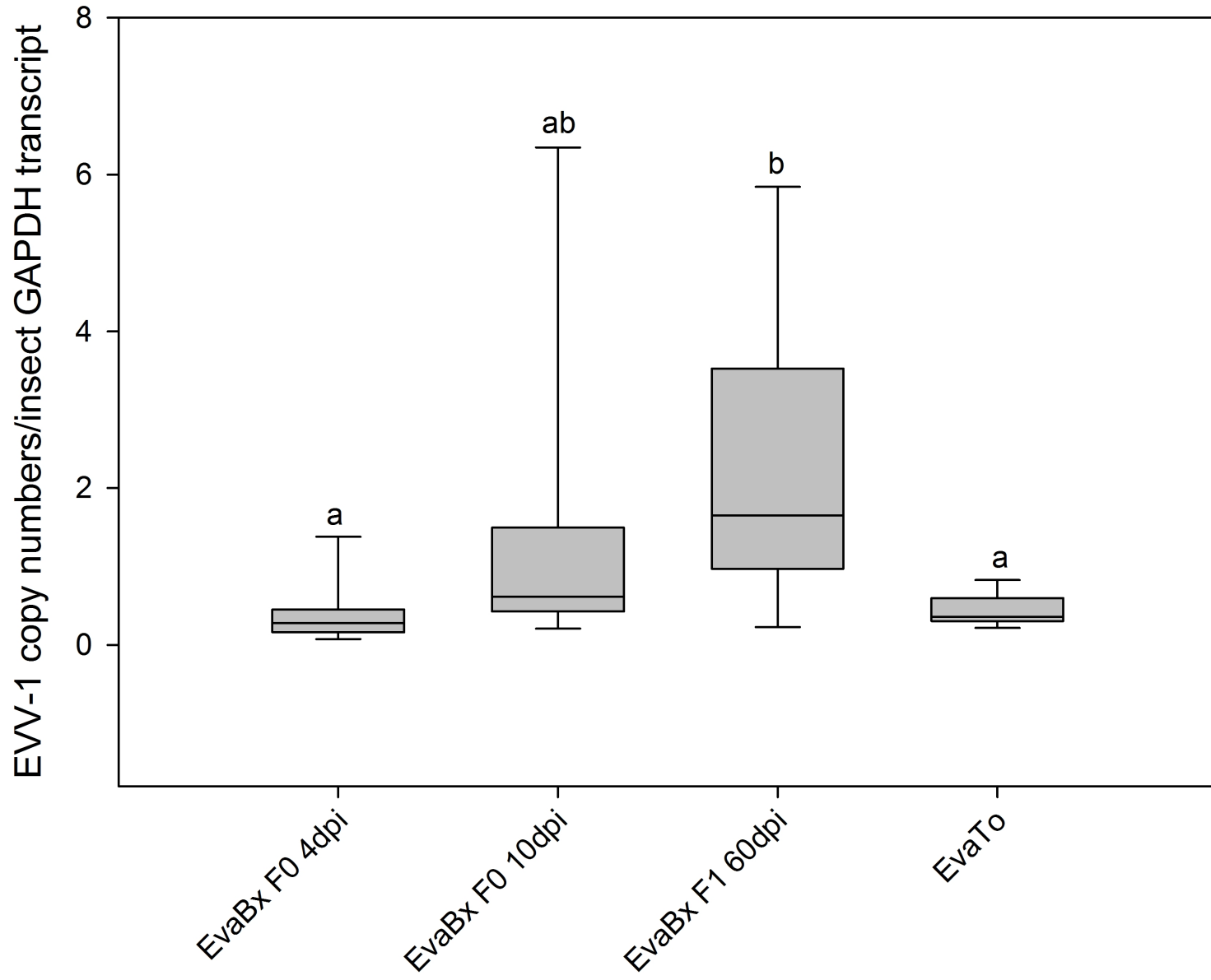
628

629 **Figure 3. Vertical transmission of *Euscelidius variegatus* virus 1 (EVV-1) injected into EVV-1
 630 free EvaBx rearing.** Different letters indicate significant differences in mean viral load
 631 measured in the sample groups. Days post injection (dpi) indicate the sampling date after
 632 viral injection. Viral load measured in infected EvaTo adults (EvaTo) was used for comparison.

633







Supplementary Tables

Supplementary Table S1. Presence and loads of *Euscelidius variegatus* virus 1 (EVV-1) in different insect life stages of the virus infected EvaTo rearing and corresponding mean transcript levels of insect glyceraldehyde-3-phosphate dehydrogenase (GAPDH). All samples were amplifiable.

Life stage	Mean EVV-1 viral load* \pm SEM (N)	Mean GAPDH transcript levels** \pm SEM (N)
Egg	944 \pm 534 (7)	848 \pm 295 (7)
1 st instar nymph	6335 \pm 654 (10)	2841 \pm 297 (10)
2 nd instar nymph	5656 \pm 638 (10)	3397 \pm 365 (10)
3 rd instar nymph	5005 \pm 289 (10)	4516 \pm 304 (10)
4 th instar nymph	3441 \pm 387 (10)	6350 \pm 541 (10)
5 th instar nymph	3045 \pm 364 (9)	6349 \pm 430 (9)
Adult Female	5810 \pm 1105 (5)	10707 \pm 254 (5)
Adult Male	3945 \pm 662 (5)	11564 \pm 1684 (5)

*Viral load expressed as EVV-1 copy numbers/ng of cDNA.

**Insect GAPDH level expressed as GAPDH transcript numbers/ng of cDNA.

Supplementary Table S2. Presence and loads of *Euscelidius variegatus* virus 1 (EVV-1) in different insect organs of the virus infected EvaTo population and corresponding mean transcript levels of insect glyceraldehyde-3-phosphate dehydrogenase (GAPDH). All samples were amplifiable.

Organs	Mean EVV-1 viral load* \pm SEM (N)	Mean GAPDH transcript levels** \pm SEM (N)
Malpighian tubules	537 \pm 185 (3)	2665 \pm 870 (3)
Salivary glands	164 \pm 36 (3)	234 \pm 41 (3)
Guts	437 \pm 66 (3)	5118 \pm 249 (3)
Ovaries	3768 \pm 1332 (5)	5491 \pm 1617 (5)
Testes	16 \pm 13 (3)	132 \pm 87 (3)
Hemolymph	741 \pm 290 (4)	57 \pm 21 (4)

*Viral load expressed as EVV-1 copy numbers/ng of cDNA.

**Insect GAPDH level expressed as GAPDH transcript numbers/ng of cDNA.

Supplementary Table S3. Presence and loads of *Euscelidius variegatus* virus 1 (EVV-1) following injection into the EVV-1 free EvaBx population. Mean quantification cycles (Cq) obtained from insect glyceraldehyde-3-phosphate dehydrogenase (GAPDH) qPCR assay confirmed that all samples were amplifiable.

Sample description	Sampling date (dpi, days post injection)	N° EVV-1 positive/ analysed samples	Mean EVV-1 viral load* \pm SEM (N)	Mean Cq \pm SEM (N) of GAPDH assay
F0 (EvaBx adults injected with EVV1 extract)	4	8/9	0.41 \pm 0.15 (8)	19.97 \pm 0.64 (9)
	10	10/10	1.37 \pm 0.63 (10)	20.20 \pm 1.49 (10)
F1 (Progeny of injected EvaBx adults)	60	16/16	2.40 \pm 0.49 (16)	17.41 \pm 0.21 (16)

*Viral load expressed as EVV-1 copy numbers/insect GAPDH transcript.